journal

J. Am. Ceram. Soc., **80** [4] 1027–31 (1997)

Hertzian Contact Damage in Porous Alumina Ceramics

Bruno A. Latella and Brian H. O'Connor

Department of Applied Physics, Curtin University of Technology, Perth, WA 6845, Australia

Nitin P. Padture*,† and Brian R. Lawn*

Materials Science and Engineering Laboratory, National Institute of Standards and Technology, Gaithersburg, Maryland 20899

A study has been made of Hertzian contact damage in porous and dense liquid-phase-sintered aluminas. Indentation stress–strain curves show increasing nonlinearity as the materials become more porous, illustrating an increasing component of "quasi-plasticity" in the contact damage. Observations of the surface and subsurface damage patterns using a bonded-interface sectioning technique reveal a transition in the Hertzian damage process, from classical tension-driven cone cracks in the high-density material, to distributed shear- and compression-driven subsurface damage and deformation in the porous materials. Strength tests on specimens subjected to cyclic indentations reveal a substantially higher susceptibility to fatigue in the most porous structure.

I. Introduction

STUDIES of Hertzian contact damage in tough monolithic and composite ceramics have revealed insights into the intrinsic role of microstructure in mechanical properties. Coarse-grained aluminas[1,2] and other heterogeneous ceramics[3–7] with high long-crack toughness show radical departures from the classical tension-driven Hertzian cone fracture typical of homogeneous fine-grained materials. This change in fracture response is most apparent in dense, coarse-grained aluminas[2] where shear-driven, distributed subsurface damage accumulation and microcracking are observed. The subsurface damage intensifies with cyclic loading, indicating fatigue tendencies, and ultimately leading to accelerated material removal. These findings have implications concerning the capacity of ceramics to sustain mechanical damage and absorb energy. They also imply that "brittle–ductile" transitions in the mechanical response of ceramics may be controlled by designed microstructural heterogeneity.

A simple fracture mechanics model of damage accumulation beneath contacts in ordinarily tough polycrystalline ceramics has been previously described.[8] Macroscopically, the damage occurs within a constrained drop-shaped zone beneath the contact area, where the stresses are highly compressive and deviatoric. At the microstructural level, the model is based on microcrack extension from stress concentrations at constrained "shear faults." In alumina, the shear faults are primarily associated with activation of intragrain twinning in a region of high compressive shear stress field beneath the contact area.[1,2] The observed microcrack density increases with grain size, implying a threshold microstructural scale for crack initiation.

In contrast, the micromechanisms controlling failure in *porous* ceramics under contact loading are not well understood. This is despite many studies on analogous processes in porous rocks.[9–14] The mechanical behavior of porous ceramics is of considerable practical importance in applications that require a high degree of porosity, e.g. filters, thermal barrier coatings, sensors, and preforms for subsequent infiltration. Accordingly, studies are being conducted to investigate low-cost processing routes for aluminas with different degrees of porosity, using readily available mineral additives.[15,16]

The specific purpose of the present study is twofold: (i) to determine experimentally the influence of porosity in liquid-phase-sintered (LPS) alumina ceramics under contact damage and fatigue conditions; and (ii) to explore the micromechanical response, and thereby gain information on the nature of the damage. LPS alumina materials with appropriate oxide additives are used to prepare specimens with up to 18% porosity. The indentation stress–strain responses in these materials exhibit enhanced quasi-plasticity with increasing porosity. Subsurface observations of contact damage in the porous materials, using a "bonded-interface" sectioning technique,[2] show clear evidence of a macroscopic damage zone. Cyclic loading tests accelerate the damage accumulation, with some indication of grain crushing, pore filling and pore collapse. Fatigue susceptibility is quantitatively assessed from strength degradation in biaxial flexure testing as a function of the number of contact cycles.

II. Experimental Procedure

Batches of powder were prepared comprising a mixture of 84 wt% alumina (Alcoa of Australia Ltd., Kwinana, Western Australia) with 9 wt% kaolinite, 5 wt% talc and 2 wt% calcite (Commercial Minerals, Kewdale, Western Australia) in deionized water. The resulting slurries were attrition-milled for 3 h and then oven-dried at 110°C for 24 h. The resulting powder cakes were crushed and screened through a 150 μm sieve. Individual batches of powder were placed in a hardened steel die and dry-pressed at 50 MPa to form disks of 30 mm diameter × 3 mm thickness. The pressed green-body specimens were then placed in high-purity alumina boats packed with loose bedding alumina powder, placed in a $MoSi_2$ resistance-heated box furnace (Model 46200, Thermolyne), and subject to one of three heat treatments in air: (a) at 1250°C for 4 h, (b) 1300°C for 1 h, or (c) 1400°C for 4 h. All specimens were cooled to room temperature at 480°C/h.

X-ray powder diffraction (XRD) determined the phase composition of the sintered aluminas, including the glassy phase, from Rietveld analysis.[15] Scanning electron microscopy (SEM) was used to examine the microstructures and to evaluate grain sizes (lineal intercept technique[17]). The bulk density of the

G. M. Pharr—contributing editor

Manuscript No. 191458. Received October 9, 1996; approved January 28, 1997.

Supported in part by an Australian Postgraduate Award at Curtin University of Technology and by the U.S. Air Force Office of Scientific Research.

*Member, American Ceramic Society.

†Now with the Department of Metallurgy and Materials Engineering, University of Connecticut, Storrs, Connecticut 06269.

Table I. Preparation and Properties of Aluminas

Sintering treatment	Porosity (%)	Grain size (μm)	Hardness (GPa)	Young's modulus (GPa)	Inert strength (MPa)
1250°C, 4 h	17.8	≈1	5.7	110	280
1300°C, 1 h	6.8	≈2	10.6	184	410
1400°C, 4 h	2.5	≈4	12.0	270	450

sintered materials was determined using Archimedes' principle.[18] The porosity was calculated from the relative density and theoretical true density value (estimated by rule of mixtures). The indentation hardness was evaluated as load/projected area from the impression diagonals of Vickers indentations using a contact load of 150 N. Young's modulus of selected specimens was determined using a time-of-flight direct transmission ultrasonic technique.

Indentation stress–strain testing[1–4] was carried out on specimens polished to a final finish with 1 μm diamond paste and then sputter coated with gold. Indentations were made using tungsten carbide (WC) spheres of radii r = 0.79, 1.19, 1.98, 3.18, 7.94, and 12.70 mm, over a load range P = 100–2500 N on a universal screw-driven testing machine (Model 1122, Instron, Canton, MA) at a constant crosshead speed (2 mm/min). Residual traces in the gold layer enabled measurement of contact radii (a). Indentation stresses ($p_0 = P/\pi a^2$) as a function of indentation strain (a/r) were then determined. For purely elastic contacts, the stress–strain relation is linear, $p_0 = (3E/4\pi k)a/r$, with E Young's modulus and k an elastic indenter/specimen coefficient.[19]

Examination of subsurface contact damage was made using a bonded-interface technique, consisting of two polished half-blocks joined together by adhesive.[2,4] Indentations were made symmetrically across the traces of the interface on a servo-hydraulic testing machine (Model 8502, Instron, Canton, MA) at specified contact loads, with a sphere of radius 3.18 mm. Single-cycle tests were conducted at loads up to 2500 N. Multiple-cycle tests were run with a sinusoidal waveform at a frequency of 10 Hz and a load of 1000 N. After testing, the bonded materials were separated and the surfaces and sections cleaned with acetone. The polished specimens were subsequently gold-coated and viewed in an optical microscope using Nomarski interference contrast to reveal the macroscopic damage patterns.

Strength degradation tests were made on polished disks of ≈22 mm diameter and 2.5 mm thickness after cyclic contact. Indentations were centered on the top surface of each disk, with a maximum contact load of 1000 N and sphere radius 3.18 mm, at a frequency of 10 Hz, over n = 1–10^5 cycles. Some specimens were left unindented for measurement of natural strengths. The disks were broken in biaxial flexure on a universal screw-driven testing machine (Model 1122, Instron, Canton, MA) with the top surface on the tension side, using a flat circular punch of diameter 3.5 mm on a three-ball support of 14.9 mm diameter.[20] A drop of silicone oil was placed on the indentation sites prior to flexure, and the specimens broken in <10 ms, to minimize environmental effects. All broken disks were examined to ensure that failure originated from the indentation sites. Those that did not were excluded from the analysis.

III. Results and Discussion

Table I summarizes the properties of the LPS materials used in this study.[15] Three levels of porosity were obtained, 2.5%, 6.8%, and 17.8%, depending on the sintering temperature and time. The XRD and SEM analyses showed that these materials all had an alumina content of ≈86 wt%, with ≈4 wt% spinel and ≈2 wt% anorthite crystalline phases, and ≈8 wt% intergranular glassy phase.

The alumina grain sizes ranged from 1 to 4 μm in the three materials.[15] In fully dense aluminas, this range is too small to have any discernible effect on the Hertzian contact response.[2] Accordingly, any effects observed below can be attributed to the porosity.

Figure 1 shows indentation stress–strain curves for single-cycle indentations in these three LPS aluminas. For reference, the inclined dashed line represents the Hertzian relation for purely elastic contacts (Section II) on the 2.5% porous material.[1] Also, the hatched boxes at the right axis represent Vickers-determined hardness values for the three materials. The curves show strikingly increasing deviations from linearity with increasing porosity, not unlike those observed in other deformable, but dense, quasi-plastic ceramics.[4]

Figure 2 shows half-surface (upper) and section (lower) views of the damage obtained in each of the LPS alumina materials from single-cycle Hertzian indentations with a sphere of 3.18 mm radius, at a peak load of 1500 N. The indentation stresses for the 2.5%, 6.8%, and 17.8% porosity materials are p_0 = 6.2, 4.3, and 3.0 GPa, respectively, i.e., just within the nonlinear regions in Fig. 1. The impression diameter and degree of subsurface damage become more pronounced with increasing porosity, consistent with the trend towards increasing quasi-plasticity in Fig. 1. The damage in the low-porosity material (Fig. 2(a)) has the form of a classical Hertzian cone fracture, with near-circular surface ring cracks and no sign of residual surface depression.[19] In the intermediate-porosity material (Fig. 2(b)), a residual depression and corresponding subsurface damage accompany the cone cracks. In the high-porosity material (Fig. 2(c)), the depression and subsurface damage are greatly enhanced, and the cone cracks reduced to surface ring cracks. Thus there is evidence of a "brittle–ductile" transition with increasing porosity, analogous to that previously observed in alumina with increasing grain size.[2] Note in the more porous materials the appearance in Figs. 2(b) and (c) of near-hemispherical fissures at the periphery of the subsurface damage zone, indicative of a material that has undergone some compaction during loading and has pulled away from the surrounds during elastic recovery on unloading.

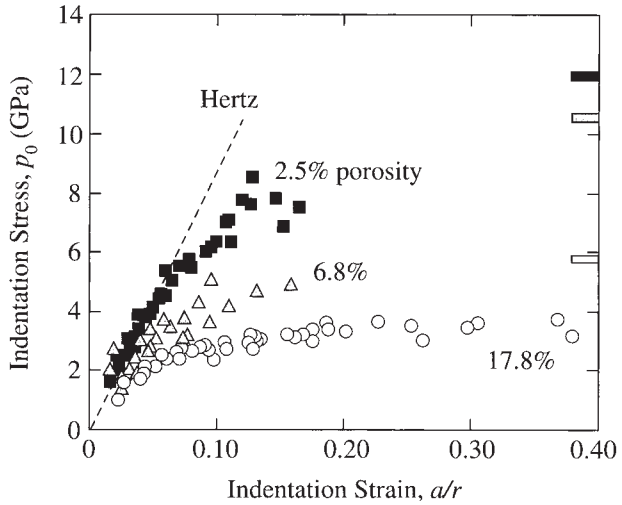

Fig. 1. Indentation stress–strain curve for single-cycle contacts for LPS aluminas of indicated porosities. Data obtained using WC spheres. Dashed line is Hertzian elastic response for 2.5% porous LPS alumina. Hatched boxes on right axis are hardness values from Vickers indentations.

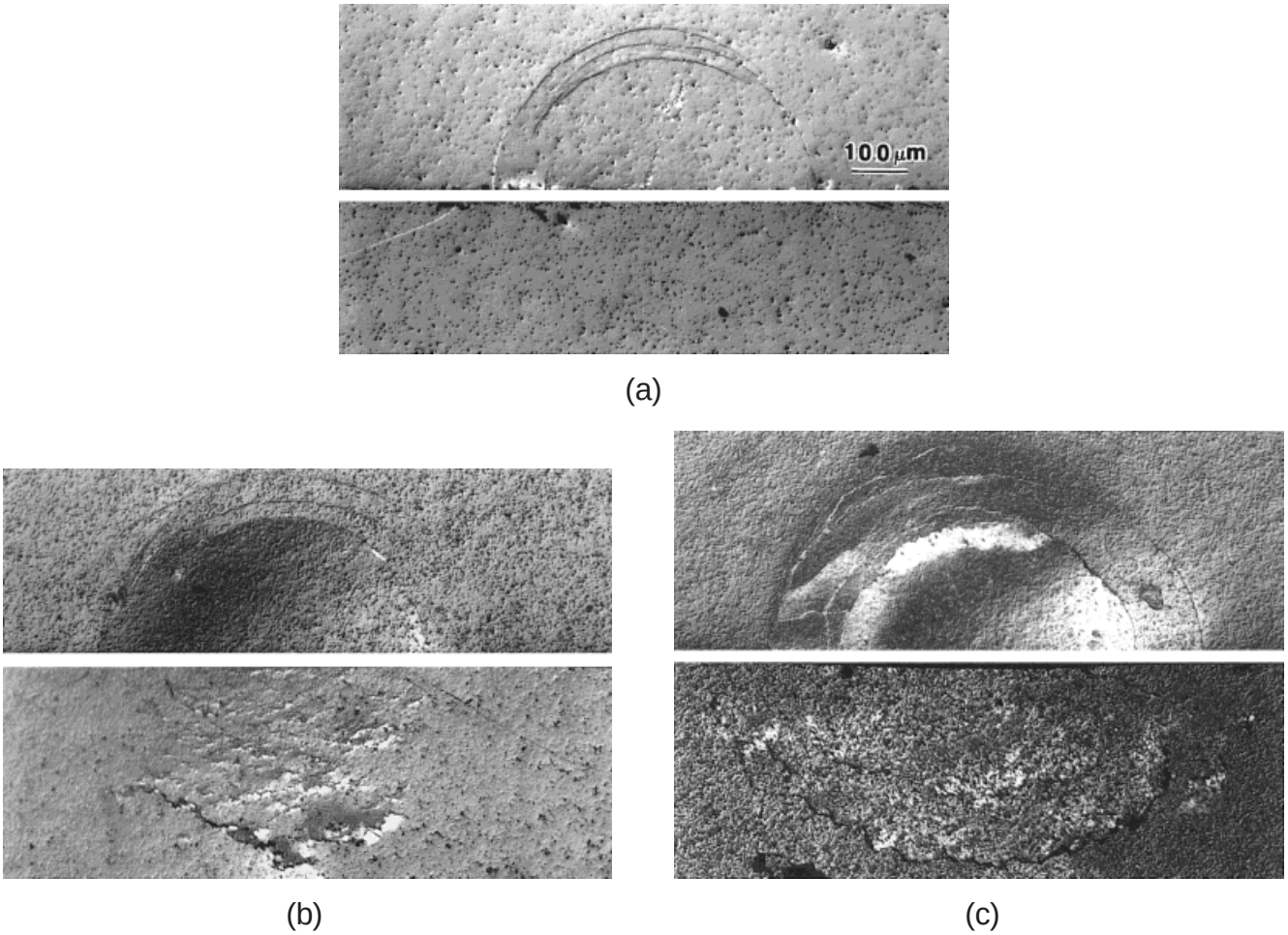

Fig. 2. Optical micrographs of Hertzian damage for LPS aluminas with porosity (a) 2.5%, (b) 6.8%, and (c) 17.8%, showing half-surface (top) and section (bottom) from bonded-interface specimens, viewed in Nomarski illumination. Single-cycle indentations produced by WC sphere, radius r = 3.18 mm, load P = 1500 N. Note fissures at periphery of deformation zones in (b) and (c).

Figure 3 shows the evolution of contact damage in each alumina material with increasing number of contact cycles, $n = 1$, 10^3, and 10^5, again with a sphere of 3.18 mm but at a lower load, 1000 N, than that in Fig. 2, in order to observe the damage buildup:

(a) For the low-porosity material (Fig. 3(a)), the damage at $n = 1$ is slight, consisting of a shallow ring crack and no subsurface deformation. After cycling at $n = 10^3$, the ring crack has extended into a cone, still without sign of subsurface damage. After $n = 10^5$, some accompanying subsurface damage is now apparent.

(b) For the intermediate-porosity material (Fig. 3(b)), the damage at $n = 1$ again begins as a shallow ring crack without subsurface deformation. After $n = 10^3$ cycles, the ring crack has extended into a cone, but now there is considerable accompanying subsurface damage. After $n = 10^5$, the cones are dominated by the subsurface damage, which is extensive to the point of material removal.

(c) For the high-porosity material (Fig. 3(c)), the damage at $n = 1$ begins as quasi-plastic deformation. After $n = 10^3$ cycles, subsurface deformation has noticeably expanded, with peripheral cracking at the zone base but without any surface ring cracking. After $n = 10^5$, the deformation zone is dramatically larger, with even more peripheral cracking, extending upward close to the specimen surface, but still without any ring cracking. Thus the more porous materials are not only more susceptible to quasi-plasticity, but also to an exaggerated damage accumulation, i.e., fatigue.

Figure 4 shows the strengths of contact damaged bend specimens of the low-porosity (2.5%) and high-porosity (17.8%) LPS aluminas as a function of number of indentation cycles n with a sphere of 3.18 mm at peak load P = 1000 N (cf. Fig. 3). Each data point represents the mean and standard deviation of at least four specimens. The strength of the low-porosity material falls abruptly by about 35% after one cycle, from failure at cone crack origins. However, this strength level does not fall significantly as n increases, indicating that the cone cracks are not highly susceptible to prolonged cyclic loading.[5] In contrast, the strength of the high-porosity material shows a relatively small falloff of about 15% after one cycle, in this case from failures at subsurface deformation origins. Thereafter, however, the strength declines dramatically with increasing n, indicating that the deformation mode is far from benign. These trends in the high-porosity material are not inconsistent with the relatively strong damage buildup noted in Fig. 3(c).

IV. Conclusion

In this study on LPS aluminas we have shown that porosity can have a dramatic influence on the nature of contact damage response of nominally brittle solids. Specifically, increasing porosity induces a transition from an essentially brittle to a quasi-plastic response in the damage mode, somewhat analogous to the influence of increasing grain size.[2] This transition is apparent both quantitatively, on indentation stress–strain curves (Fig. 1), and qualitatively, on ceramographic sections (Fig. 2). The quasi-plastic damage in particular is susceptible to mechanical fatigue,

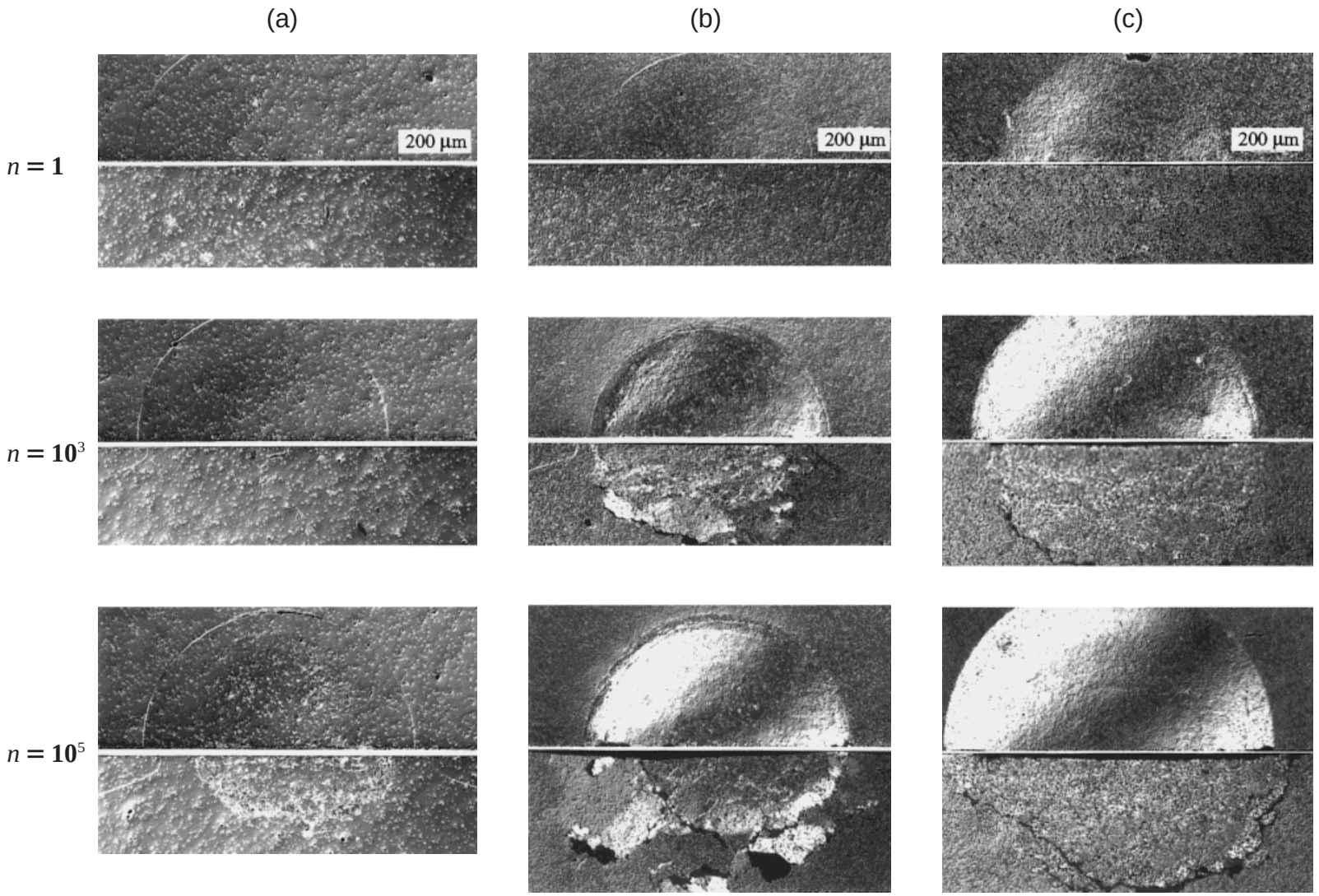

Fig. 3. Optical micrographs of Hertzian damage for LPS aluminas with porosity (a) 2.5%, (b) 6.8%, and (c) 17.8%, showing half-surface (top) and section (bottom) from bonded-interface specimens, viewed in Nomarski illumination. Multiple-cycle indentations at $n = 1$, 10^3, and 10^5 produced by WC sphere, radius $r = 3.18$ mm, load $P = 1000$ N, at 10 Hz.

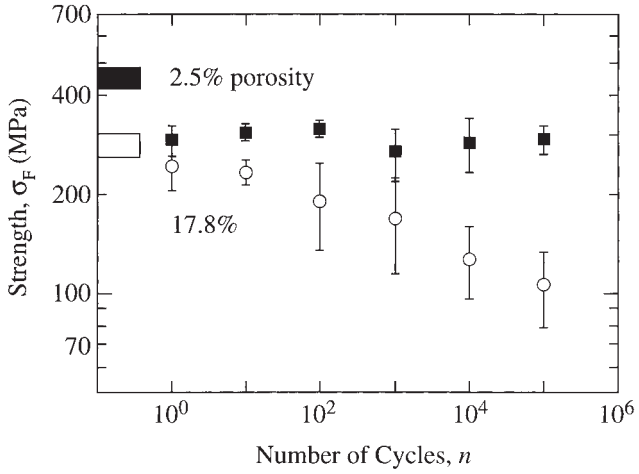

Fig. 4. Inert strength as a function of number of indentation cycles for LPS aluminas with 2.5% and 17.8% porosity. Error bars are standard deviations (minimum four specimens).

as revealed in the micrographs (Fig. 3) and on strength degradation curves (Fig. 4).

This influence of porosity on indentation stress–strain behavior and contact damage response has serious implications concerning the capacity of ceramics to sustain mechanical damage and to absorb energy in impacts. The results indicate that the performance of ceramic-based structures may be controlled by the level of porosity, and hence by processing strategies. Such is the case with porous coatings for thermal barriers,[21] ceramic preforms for glass infiltration,[22] and porous ceramic matrices for damage-tolerant composites,[23] where porosity and other defect content is paramount to the mechanical response. This raises the prospect of designing low-cost aluminas and other ceramics for applications where flaw tolerance, thermal shock, thermal resistance, energy absorption and permeability are major interests.

The present study leaves unanswered questions concerning the underlying nature of the quasi-plastic damage in the porous structures. In most tough ceramics the quasi-plasticity is identifiable with internal shear-driven defects with friction at sliding interfaces, so-called "shear faults."[7,8] In the present case there is a strong indication that compaction plays a major role in the deformation, possibly by structural breakdown and subsequent intrusion of material into the pores (pore collapse, or "cataclastic flow")[11] or by growth and coalescence of interpore cracks.[14] The specific mechanisms of such deformation are a relatively unexplored area in ceramics.

Acknowledgments: Thanks are due to J. Lochore of Alcoa of Australia Ltd. for providing the alumina powder, and S. Darby for assistance with specimen preparation at NIST.

References

[1]F. Guiberteau, N. P. Padture, H. Cai, and B. R. Lawn, "Indentation Fatigue: A Simple Cyclic Hertzian Test for Measuring Damage Accumulation in Polycrystalline Ceramics," *Philos. Mag. A*, **68** [5] 1003–16 (1993).

[2]F. Guiberteau, N. P. Padture, and B. R. Lawn, "Effect of Grain Size on Hertzian Contact in Alumina Ceramics," *J. Am. Ceram. Soc.*, **77** [7] 1825–31 (1994).

[3]H. Cai, N. P. Padture, B. M. Hooks, and B. R. Lawn, "Flaw Tolerance and Toughness Curves in Two-Phase Particulate Composites: SiC/Glass System," *J. Eur. Ceram. Soc.*, **13**, 149–57 (1994).

[4]H. Cai, M. A. Stevens Kalceff, and B. R. Lawn, "Deformation and Fracture of Mica-Containing Glass-Ceramics in Hertzian Contacts," *J. Mater. Res.*, **9** [3] 762–70 (1994).

[5]N. P. Padture and B. R. Lawn, "Contact Fatigue of a Silicon Carbide with a Heterogeneous Grain Structure," *J. Am. Ceram. Soc.*, **78** [6] 1431–38 (1995).

[6]H. H. K. Xu, L. Wei, N. P. Padture, B. R. Lawn, and R. L. Yeckley, "Effect of Microstructural Coarsening on Hertzian Contact Damage in Silicon Nitride," *J. Mater. Sci.*, **30**, 869–78 (1995).

[7]B. R. Lawn, N. P. Padture, H. Cai, and F. Guiberteau, "Making Ceramics 'Ductile,' " *Science*, **263**, 1114–16 (1994).

[8]B. R. Lawn, N. P. Padture, F. Guiberteau, and H. Cai, "A Model for Microcrack Initiation and Propagation Beneath Hertzian Contacts in Polycrystalline Ceramics," *Acta Metall. Mater.*, **42** [5] 1683–93 (1994).

[9]J. C. Jaeger and N. G. W. Cook, *Fundamentals of Rock Mechanics*. Chapman and Hall, London, U.K., 1971.

[10]J. Zhang, T.-F. Wong, and D. M. Davis, "Micromechanics of Pressure-Induced Grain Crushing in Porous Rocks," *J. Geophys. Res.*, **95** [B1] 341–52 (1990).

[11]G. Hirth and J. Tullis, "The Effects of Pressure and Porosity on the Micromechanics of the Brittle–Ductile Transition in Quartzite," *J. Geophys. Res.*, **94** [B12] 17825–38 (1989).

[12]J. T. Fredrich, B. Evans, and T.-F. Wong, "Micromechanics of the Brittle to Plastic Transition in Carrara Marble," *J. Geophys. Res.*, **94** [B4] 4129–45 (1990).

[13]T.-F. Wong, "Mechanical Compaction and the Brittle–Ductile Transition in Porous Sandstones"; pp. 111–22 in Geological Society Special Publication, No. 54, *Deformation Mechanisms, Rheology and Tectonics*. Edited by R. J. Knipe and E. H. Rutter. Geological Society of London, Oxford, U.K., 1990.

[14]C. G. Sammis and M. F. Ashby, "The Failure of Brittle Porous Solids Under Compressive Stress States," *Acta Metall.*, **34** [3] 511–26 (1986).

[15]B. A. Latella, "Development of Debased Alumina Wear-Resistant Ceramics"; Ph.D. Thesis. Curtin University of Technology, Perth, W.A., Australia, 1995.

[16]J. Carter, "Development of Reaction-Sintered Alumina-Matrix Ceramics"; Ph.D. Thesis. Curtin University of Technology, Perth, W.A., Australia, 1995.

[17]J. C. Wurst and J. A. Nelson, "Lineal Intercept Technique for Measuring Grain Size in Two-Phase Polycrystalline Ceramics," *J. Am. Ceram. Soc.*, **55** [2] 109 (1972).

[18]Australian Standard 1774.5, *Refractories and Refractory Materials—Physical Test Methods. Method 5: The Determination of Density, Porosity and Water Absorption*; pp. 1–4. Standards Australia, Sydney, Australia, 1989.

[19]F. C. Frank and B. R. Lawn, "On the Theory of Hertzian Fracture," *Proc. R. Soc. London*, **A229**, 291–306 (1967).

[20]D. B. Marshall, "An Improved Biaxial Flexure Test for Ceramics," *Am. Ceram. Soc. Bull.*, **59** [5] 551–53 (1980).

[21]A. Pajares, L. Wei, B. R. Lawn, and C. C. Berndt, "Contact Damage in Alumina-Based Plasma Sprayed Coatings," *J. Am. Ceram. Soc.*, **17** [7] 1907–14 (1996).

[22]W. D. Wolf, K. J. Vaidya, and L. F. Francis, "Mechanical Properties and Failure Analysis of Alumina–Glass Dental Composites," *J. Am. Ceram. Soc.*, **79** [7] 1769–76 (1996).

[23]W.-C. Tu, F. F. Lange, and A. G. Evans, "Concept for a Damage-Tolerant Ceramic Composite with 'Strong' Interfaces," *J. Am. Ceram. Soc.*, **79** [2] 417–24 (1996). □